



Pyrolysis method. Spray pyrolysis can solve these issues by precisely controlling cell components and improving efficiency. The technique also enables using less expensive materials, thereby increasing economic viability. DSSC technology can be developed and used more quickly with spray pyrolysis, which also solves many of the problems in the field [14].

Solar cells that collect solar electricity are typically categorised according to their material composition, including organic dye solar cells, dye-sensitized, non-crystal, multiple-crystal, and single-crystal silicon solar cells [15]. Spray pyrolysis is being continuously enhanced to enhance solar cells' quality. In the following applications, spray pyrolysis techniques are currently employed, i.e. conventional deposition, thin film deposition, jet nebuliser, flame spray, jet ultrasonic, laser pyrolysis, and electrospray [15]. There are several benefits to this procedure, including the easy way to dope films by adding certain materials and the fact that it is done in the air. Operating at lower temperatures makes manufacturing compact and straightforward [16]. Spray pyrolysis deposits useful thin films and coatings on diverse surfaces using a unique gas-phase growth process. It is a versatile technique for applying thin films in various applications, including DSSC. Mathematical descriptions of the main principles of spray pyrolysis can be used to understand the relationship between different operational factors and the deposition rate or film thickness. This relationship is given in Eq. (1):

$$R = \eta \frac{CV}{A} \quad (1)$$

where  $R$  is the deposition rate (thickness per unit time),  $\eta$  is the deposition efficiency,  $C$  is the precursor solution concentration,  $V$  is the volumetric flow rate of the solution, and  $A$  is the area over which the solution is sprayed.

In spray pyrolysis, solid or liquid feed materials are pumped into a reactor and heated using flame or plasma to give a high-temperature gas. These rapidly moving gases deposit a thin film from a gaseous phase in a process called Physical Vapor Deposition. Spray pyrolysis has many advantages, including the flexibility to produce various thin film materials. The methods used to create the coating include metals, ceramics and oxides. It also has an impressive scalability for small-scale prototypes to large-scale manufacture [1]. Moreover, the spray pyrolysis technique possesses the great advantage of being a very efficient process with a high deposition rate. It is an excellent alternative for applications needing a fast and effective coating process. Spray pyrolysis is widely used for the coating of high-temperature and high-heat-resistant materials. It can help save the environment by creating non-toxic and non-polluting coatings. Spray pyrolysis is a promising surface coating technology that provides a versatile and effective coating method for different applications [18, 19]. As discussed earlier, one of the coating technologies applied in this study is spray pyrolysis, enhanced explicitly by integrating intelligent spray pyrolysis using NodeMCU [20]. Therefore, this study intends to provide an inexpensive solution using IoT tools like the NodeMCU side-by-side, which can be implemented into the full-fledged implementation hardware later. NodeMCU is a line of low-cost open-source hardware that uses the ESP8266 microchip and is able to connect to a Wi-Fi network and control electronic devices wirelessly. It is broadly used in many IoT applications such as automation, remote sensing and home intelligent devices [20, 21]. This work presents a new approach to applying IoT technology in the manufacturing process of DSSCs aimed at lowering production costs and enhancing film deposition process control and uniformity.

In this study, the NodeMCU was adopted for spray pyrolysis, allowing remote control via a Wi-Fi connection. This involved regulating the pyrolysis process temperature and flow rate, monitoring the performance of the coating and entering data in a machine-readable format for analysis. The NodeMCU also controls and monitors several processes or equipment, including pumps, valves, and temperature sensors in laboratory or industrial settings. This facilitated remote tracking and control of the Spray Pyrolysis process, which has significantly helped us in specific applications. In this study, the NodeMCU-controlled spray on-and-off time connection was through a hotspot connection. In this study, the IoT-based controller was successfully used to obtain the optimal thickness of  $\text{TiO}_2$  solution with different volumes at the heights of 8 cm, 12 cm and 16 cm, leading to even/consistent coatings. This new technique of deposition uniformity improved DSSC performance, overcoming some issues associated with manually sprayed films, which resulted in non-uniform surfaces.

## 2. MATERIAL AND METHODS

### 2.1 Preparation of $\text{TiO}_2$ Solution

The anatase was obtained during the preparation by pulverizing about 0.3 g of commercial Degussa P25 powder in a mortar. Then, 5.5 ml of acetic acid was dissolved separately in a beaker and mixed properly. After that, 20 ml of TKC-302 was added to the mortar, stirred well, and poured into a light-resistant bottle. As a solvent and surfactant, 30 ml ethanol and five drops of Triton X-100 were added to the bottle. After that, the container was placed in an ultrasonic device and processed for half an hour.

### 2.2 Masking Process for Conductive Glass

The conductive area of FTO glass was masked according to the needed shape before depositing  $\text{TiO}_2$  solution onto the FTO glass. In the current study, we used two types of masking: square and round. The area covered by a round mask was  $0.25 \text{ cm}^2$ , and the area covered by a square mask was  $1 \text{ cm}^2$ . To provide uniform and reproducible results, mask

deposition of the TiO<sub>2</sub> solution was applied. After masking, The FTO glass was cleaned, removing residues that might have affected adhesion or conductivity. The masked regions are shown in Figure 1.

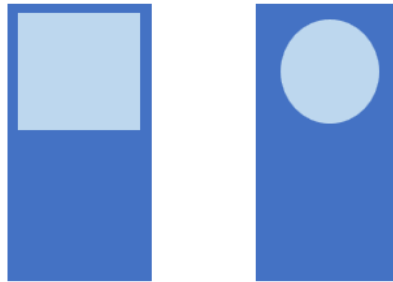


Figure 1. Illustration of masking in square and circular shapes

### 2.3 Deposition of TiO<sub>2</sub> Solution on FTO using Spray Pyrolysis Deposition Method

The solution was poured into the spray container, and the cleaned FTO glass substrates were placed on a hot plate to initiate the spray process. The glass substrate was maintained at 150 °C during the deposition to ensure even coating. Each spray lasted for 10 seconds, allowing the solution to settle uniformly. This process was repeated until the solution in the spray tank was depleted. Subsequently, the coated glass substrates were annealed in a furnace at 450 °C for 1 hour to enhance the film's properties. A spray nozzle is used in the spray pyrolysis method by incorporating an IoT system. The input of this system is by using the push button and the slider in the Blynk application. The control unit is NodeMCU ESP32, and the output is a servo motor to turn on the Airbrush. Figure 2 shows the Block Diagram of the hardware. The NodeMCU ESP32 is crucial in spray pyrolysis for accurate regulation and mechanization. The system controls many factors, such as the length and rate of spraying, monitors temperature and pressure, and automates the process to guarantee consistent and high-quality thin films. Moreover, it facilitates the recording of data for analysis. It enables the capacity to monitor and manage the spray pyrolysis process from a distance, hence improving the efficiency and dependability of the process.

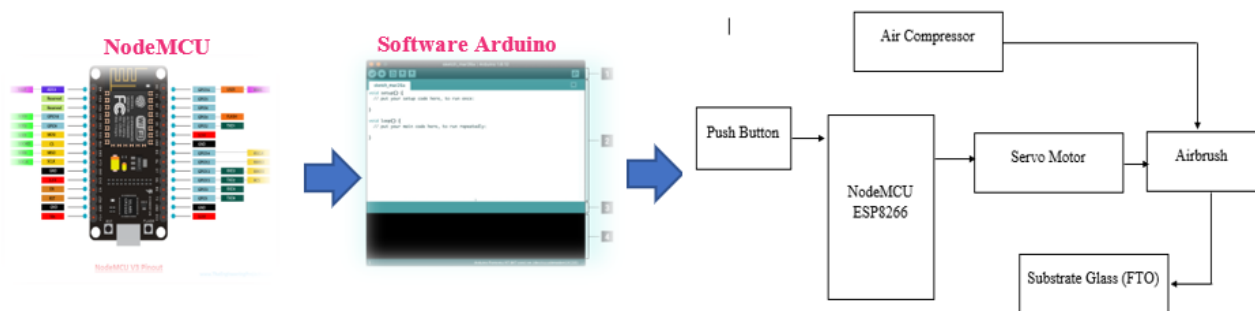


Figure 2. Block diagram of the automated spray pyrolysis system

### 2.4 Soaking Process

Following TiO<sub>2</sub> semiconductor fabrication through spray pyrolysis, the coated FTO glass substrates were immediately immersed into a dye solution to sensitize the films. In the present study, the sensitization was carried out using a synthetic dye, N719. The immersion was done in a closed container at room temperature for 24 hours for proper dye absorption. This step is essential since it helps the dye molecules bind securely to the TiO<sub>2</sub> surface, enabling efficient light absorption and flow of electrons, which play a vital role in DSSC performance.

### 2.5 Characterization and Analysis

Three characterization methods were conducted on the prepared samples. The surface morphology and microstructure of the TiO<sub>2</sub> films were examined by Field Emission Scanning Electron Microscopy (FE-SEM, JEOL JSM-7600F). The formation of uniform and dense coating deposition on the metal surface indicated that parameters such as surface evenness and film thickness are promising indicators for the quality of the coating. X-ray Diffraction Analysis (XRD) was used to analyze the crystal structure of the TiO<sub>2</sub> films. This is relevant to investigate the phase composition, crystallite size, and crystallinity, as they directly correlate to the structural attributes of the material and its impact on DSSC performance. DSSCs were characterized in terms of photovoltaic performance through IV measurement. The efficiency of the solar cells was determined by measuring parameters such as open-circuit voltage, short-circuit current density, fill factor, and overall conversion efficiency.

### 3. RESULTS AND DISCUSSION

#### 3.1 Structural Properties of TiO<sub>2</sub> used X-Ray Diffraction

The structure of materials is determined using XRD. In the case of TiO<sub>2</sub>, it can be used to identify the crystal structure and phase of the material. According to the peak intensity of the sample, the nanoparticles that were generated are crystalline, and the broad diffraction peaks indicate that the size of crystallites is relatively small. The graph visually illustrates TiO<sub>2</sub> anatase and rutile. This is due to the presence of those phases in materials that utilise titanium (IV), isopropoxide (TTP) and Degussa P25 (company product) [22].

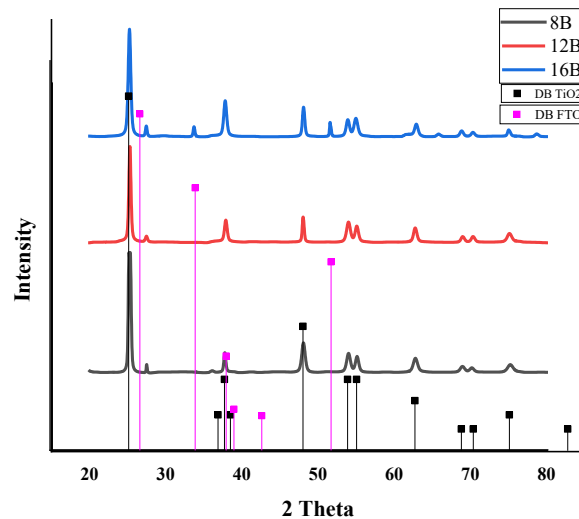


Figure 3. XRD patterns of (a) TiO<sub>2</sub> anatase (JCPDS card no. 21-1272), (b) TiO<sub>2</sub> rutile (JCPDS card no. 21-1276) and (c) FTO

It was determined that the crystallite size of the film was approximately 30.88 nm and 43.21 nm for a height of 8 cm, 27.01 nm and 38.47 nm for a height of 12 cm, and 21.61 nm and 144.82 nm for a height of 16 cm, using Scherrer's equation. Table 1 shows the numerical results of crystal sizes at various heights, indicating that the outcomes of those crystal sizes are slightly comparable and that all three display crystallinity. This suggests that the sample was not amorphous. The XRD was employed to ascertain the presence of TiO<sub>2</sub> in three samples, as illustrated in Figure 3. It has been noted that the highest intensity and presence of TiO<sub>2</sub> are observed at a height of 12 cm. The sample prepared at a height of 12 cm demonstrated the highest peak intensity compared to those prepared at heights of 8 cm and 16 cm. This maximal intensity indicates a unit cell containing the largest atoms and electrons within the studied material. Furthermore, the observed broadening of the peak is often attributed to a reduction in crystallite size, as smaller crystallites tend to increase diffraction peak width.

Table 1. Calculation of crystal size

Height	Position (2Th.)	Intensity (%)	FWHM (Full Width at Half Maximum) (Beta)	Crystallite size D (nm)
8 cm	25.3472	100.00	0.2755	30.88
	25.1359	94.16	0.1968	43.21
12 cm	25.2760	100.0	0.3149	27.01
	48.0094	30.26	0.2362	38.47
16 cm	25.2210	100.00	0.3936	21.61
	27.4499	10.44	0.0590	144.82

#### 3.2 Morphological Properties of TiO<sub>2</sub> Thin Films

Figure 4 depicts surface morphology with the same sample but varying thicknesses and heights. As indicated by the visual above, the magnification is 50000 times. The height parameter from discharge to the substrate is 8 cm for the sample in Figure 4(a). The sample is agglomerated; however, the nanoparticle does not appear optimistically. It showed good details but low porosity and irregular FTO glass. Under the previous study [23], the increased absorption results from the uniform and appropriate thickness of TiO<sub>2</sub> on a substrate, which is due to the formation of more pores. This is because the height impacted the deposition solution on the substrate. Compared to the sample shown in Figure 4(b), where the spray height to the substrate is 12 cm, the sample exhibits agglomeration and well-defined nanoparticles, resulting in a more uniform surface than the other samples. On the other hand, the TiO<sub>2</sub> surface morphology in Figure 4(c) resembles

that of Figure 4(a). However, the nanoparticles are not fully visible. Additionally, the resulting image differs from the previous samples, displaying a more porous structure, which can enhance light absorption.

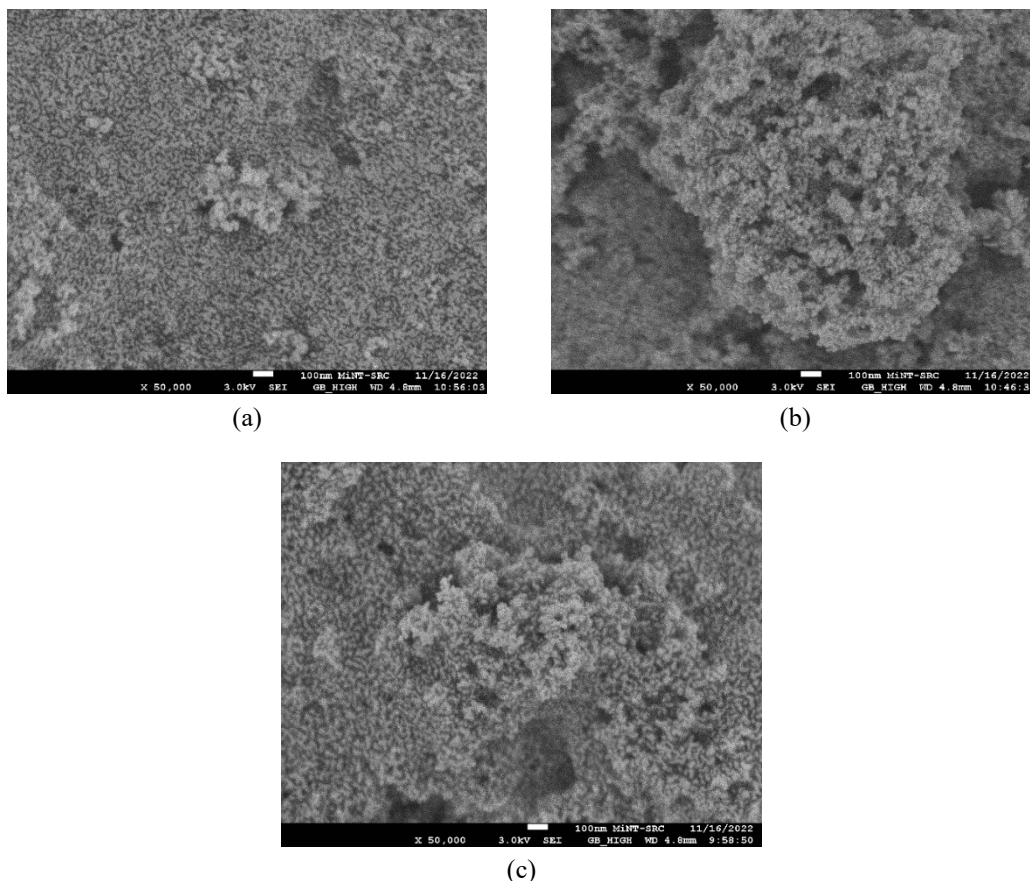


Figure 4. FE-SEM images of  $\text{TiO}_2$  surface: (a) 8 cm, (b) 12 cm and (c) 16 cm

The three Field Emission Scanning Electron Microscopy images (refer to Figure 4) exhibit a relatively large surface area for the  $\text{TiO}_2$  surface with a height of 12 cm compared to the 8 cm and 16 cm samples. The efficiency of the DSSC is improved by a higher  $J_{sc}$ , which results from a wider surface area [24]. Additionally, the spherical shape of the surface (pores) contributes to this enhancement by enabling more effective pigment (sensitizer) absorption. This issue is closely related to I-V measurement data to determine DSSC performance. The 8 cm and 16 cm heights have a surface area shape similar to pores. However, the surface layer turns thin if the spray nozzle is too far from the sample. Atomic defects and a significant decrease in DSSC performance may result from forming fractures in the layer if the distance between the spray nozzle and the sample is excessively close. Also, the probability of dye degradation will be elevated due to the difficulty of dye absorption.

### 3.3 I-V Measurement

The I-V measurement and efficiency calculations for DSSC fabricated using the spray pyrolysis method offer valuable insight into the cell performance characteristics. Under solar illumination, the maximum voltage that can be generated by such a cell is theoretically equivalent to the difference between the redox potential of the electrolyte and the (quasi-) Fermi level of the  $\text{TiO}_2$ , which is approximately 0.7 V. If an illumination DSSC were connected to a voltmeter in an open circuit, the reading would be in the same result. DSSC has a voltage  $V_{oc}$  of 0.7 to above 0.6 V, higher than silicon [24].

Table 2. I-V performance of height variation for  $\text{TiO}_2$ - Dye N719

Height (cm)	$V_{oc}$ (V)	$I_{sc}$ (mA/cm <sup>2</sup> )	Fill Factor	Efficiency (%)
8 cm	0.818	0.0035	56.59	6.54
12 cm	0.802	0.0083	43.79	11.77
16 cm	0.789	0.0087	35.67	9.74
Manual spray (12 cm)	0.806	0.0031	74.67	7.55

In a previous study that used  $\text{TiO}_2$  with a different fabrication method, spin coating followed by immersion in N719 dye achieved a DSSC efficiency of 0.0222% [25]. Another study employing the screen-printing method reported efficiencies of 7.03% and 2.78%, respectively [26]. The significant improvement in efficiency found in the current

research indicates that the parameters employed, specifically the spray height and annealing temperature of 450 °C are crucial for optimizing the performance of DSSC. This study achieved the highest efficiency at a spray height of 12 cm, with an efficiency of 11% (Figure 5). This is why, in this study, spray pyrolysis was employed. The technique is one of the most promising since it can be used to create thin films on a large scale. The optimal distribution of the TiO<sub>2</sub> solution at this height is responsible for the outcome, which is more uniform and well-structured. The even deposition likely facilitated improved dye adsorption and electron transport, leading to a higher photocurrent and, as a result, an increase in efficiency [27]. In addition, the open-circuit voltage  $V_{oc}$  values recorded in this investigation, ranging from 0.789 V to 0.818 V, align with the anticipated  $V_{oc}$  for DSSC. The more elevated  $V_{oc}$  values found in this study suggest effective charge separation and minimized recombination inside the cell, hence contributing to high efficiency. However, it is crucial to acknowledge the decline of the fill factor as the spray height increases. This indicates that although a greater spray height may enhance specific characteristics of the film, such as uniformity and thickness, it may also introduce defects or non-ideal structures that harm the cell's overall performance [28].

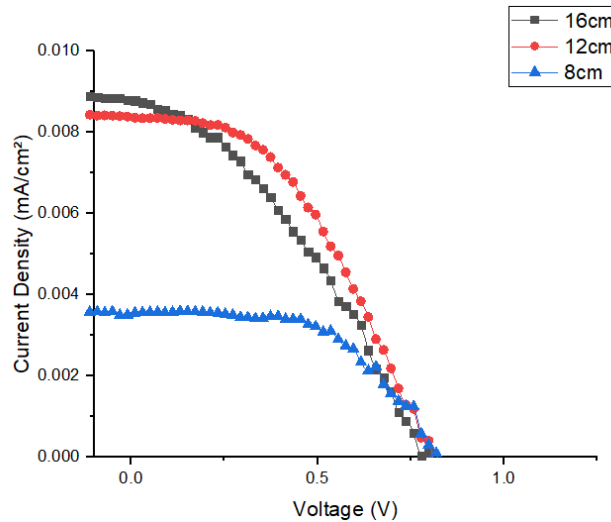


Figure 5. I-V measurement of TiO<sub>2</sub> thin film with different height

According to Table 2, the highest efficiency value is achieved at a height of 12 cm. An additional experiment was conducted using manual spray (using hand) to compare at the same height. This experiment obtained a lower efficiency value of 7.55% (see Figure 6). The decline in efficiency can be attributed to several variables, such as unstable distances. When using hands unconsciously, the position of the distance must be adjusted intermittently, either higher or lower. This can lead to uneven particle accumulation and subsequent aggregation [17]. Another factor is the inappropriate timing of the on and off spray intervals, resulting in an uneven evaporation process. This contrasts with spray pyrolysis, which Blynk Software can control to ensure consistent parameters.

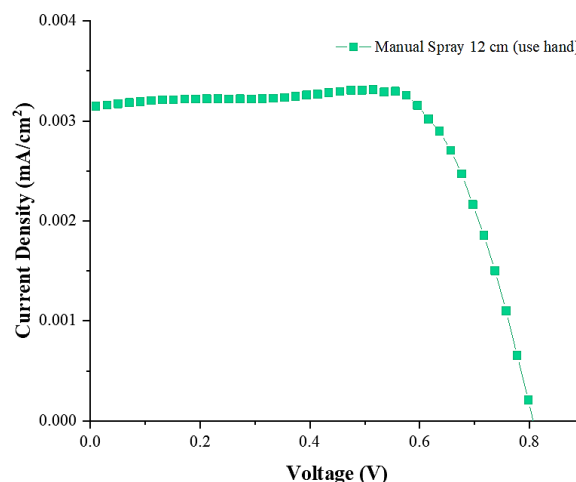


Figure 6. I-V measurement of TiO<sub>2</sub> thin film using the manual spray with a height of 12 cm

The results of this investigation illustrate the efficiency of spray pyrolysis in creating TiO<sub>2</sub> thin films in DSSC. Spray pyrolysis offers unique advantages, such as cost efficiency, scalability, and precise film thickness and structure control, in contrast to other methods, such as spin coating and screen printing. The potential of spray pyrolysis to produce high-quality films with minimal defects and an ideal thickness is demonstrated by the high efficiency obtained in DSSC fabricated with a 12 cm spray height. This uniformity enhances the performance of DSSC by enhancing light absorption

and electron transport. The production of multiple samples is restricted by the lack of a movable spray nozzle in the control system despite the numerous benefits of spray pyrolysis. The goal is to make a 3D smart spray device that can move in different directions. This system's subject is a spray mechanism that can move along two or more axes (e.g., horizontal and vertical dimensions), allowing for precise control over the spraying process. This 3D spray system will enable the production of numerous samples with homogeneous layers and the desired thickness, thereby enhancing the quality and consistency of the coatings.

#### 4. CONCLUSIONS

This study investigates the impact of an IoT-based controller on spray pyrolysis, a method utilised to fabricate TiO<sub>2</sub> semiconductors at varying heights of 8 cm, 12 cm, and 16 cm. The results suggest that an optimum efficiency of 11% is achieved at a spray height of 12 cm. The product's increased performance results from the precise regulation of the spraying process. This is achieved by minimising agglomeration and improving surface evenness. Controlling the time on and off is possible with the help of the Internet of Things. However, when manual spraying was performed at a height of 12 cm, the efficiency was reduced because the surface deposition area was uneven. This emphasises the need for process control to maximise the performance of DSSCs. The results highlight the capability of IoT technology to enhance the manufacturing process of DSSCs, resulting in more reliable and higher-performing devices. Although manual spray can be controlled to move in all directions, it is still possible that there will be different thicknesses in certain areas due to instability in the hand. Therefore, in the future, a 3D smart spray can be made using the same manufacturing concept as an IoT-based smart spray control system that can move in all directions and be controlled via devices such as laptops and cell phones.

#### ACKNOWLEDGEMENT

This research was supported by Universiti Tun Hussein Onn Malaysia (UTHM) through Tier 1 (vot Q550).

#### CONFLICT OF INTEREST

The authors declare no conflicts of interest to report regarding the present study.

#### AUTHORS CONTRIBUTION

D. G. Saputri (Conceptualization; Formal analysis; Writing - original draft; Writing - review & editing)

M. Z. N. Azmi (Methodology; Data curation; Writing - original draft)

M. K. Ahmad (Visualisation; Supervision; Resources)

A. Supriyanto (Visualisation; Supervision; Methodology)

A. B. Faridah (Visualisation; Supervision; Methodology; Data curation; Formal analysis)

A. M. S. Nurhaziqah (Investigation; Resources; Software)

A. R. Shazleen (Resources; Formal analysis)

N. K. Abd Hamed (Data curation; Formal analysis; Investigation)

A. D. Sutomo (Supervision; Methodology)

N. M. A. N. Ismail (Funding acquisition; Project administration; Supervision)

#### AVAILABILITY OF DATA AND MATERIALS

The data supporting this study's findings are available on request from the corresponding author.

#### ETHICS STATEMENT

Not applicable

#### REFERENCES

- [1] M. Okuya, N. A. Prokudina, K. Mushika, S. Kaneko, "TiO<sub>2</sub> thin films synthesized by the spray pyrolysis deposition (SPD) technique," *Journal of the European Ceramic Society*, vol. 19, no. 6–7, pp. 903-906, 1999.
- [2] G. P. Smestad, F. C. Krebs, C. M. Lampert, C. G. Granqvist, K. L. Chopra, X. Mathew, et al., "Reporting solar cell efficiencies in solar energy materials and solar cells," *Solar Energy Materials and Solar Cells*, vol. 92, no. 4, pp. 371-373, 2008.
- [3] K. Moore, W. Wei, "Applications of carbon nanomaterials in perovskite solar cells for solar energy conversion," *Nano Materials Science*, vol. 3, no. 3, pp. 276-290, 2021.
- [4] M. Gratzel, "Dye-sensitized solar cells," *Journal of Photochemistry and Photobiology C: Photochemistry Reviews*, vol. 4, no. 2, pp. 145-153, 2003.



- [5] A. Supriyanto, D. G. Saputri, M. K. Bin Ahmad, A. H. Ramelan, F. Ramadhani, "Significant efficiency improvement of TiO<sub>2</sub>:LEG4-Ag layer dye sensitized solar cells by incorporating small concentration of Ag," *Optik*, vol. 231, p. 166429, 2021.
- [6] A. Supriyanto, D. G. Saputri, M. K. Bin Ahmad, A. D. Sutomo, A. H. Ramelan, "Influence of coating a TiO<sub>2</sub> electrode with DN-F05 and DN-F05-Ag on the photovoltaic performance of DSSC solar cells," *Applied Sciences*, vol. 13, no. 13, p. 7459, 2023.
- [7] F. A. Unal, S. Ok, M. Unal, S. Topal, K. Cellat, F. Şen, "Synthesis, characterization, and application of transition metals (Ni, Zr, and Fe) doped TiO<sub>2</sub> photoelectrodes for dye-sensitized solar cells," *Journal of Molecular Liquids*, vol. 299, p. 11277, 2020.
- [8] A. Okello, B. O. Owuor, J. Namukobe, D. Okello, J. Mwabora, "Influence of concentration of anthocyanins on electron transport in dye sensitized solar cells," *Heliyon*, vol. 7, no. 3, p. e06571, 2021.
- [9] J. A. Castillo-Robles, E. Rocha-Rangel, J. A. Ramírez-De-león, F. C. Caballero-Rico, E. N. Armendáriz-Mireles, "Advances on dye-sensitized solar cells (DSSCs) nanostructures and natural colorants: A review," *Journal of Composites Science*, vol. 5, no. 11, p. 288, 2021.
- [10] A. Omar, M. S. Ali, N. Abd Rahim, "Electron transport properties analysis of titanium dioxide dye-sensitized solar cells (TiO<sub>2</sub>-DSSCs) based natural dyes using electrochemical impedance spectroscopy concept: A review," *Solar Energy*, vol. 207, no. 1, pp. 1088-1121, 2020.
- [11] A. Supriyanto, A. H. Ramelan, M. K. Bin Ahmad, F. Ramadhani, D. G. Saputri, "Hubungan sifat optik terhadap performa kinerja sel surya DSSC transparan berbahan dye DN-F01 sebagai sensitizer," *Indonesian Journal of Applied Physics*, vol. 10, no. 2, pp. 163-170, 2020.
- [12] U. Diebold, "The surface science of titanium dioxide," *Surface Science Reports*, vol. 48, no. 5-8, pp. 53-229, 2003.
- [13] E. Supriyanto, L. Ni'mah, S. Sujito, N. Alviati, A. Dikayanti, A. G. E. Sutjipto, "Optimization of TiO<sub>2</sub>/Ag photoanode thickness for improvement dye-sensitized solar cell (DSSC) performance with simulation method," in *AIP Conference Proceedings*, vol. 2682, p. 030002, 2023.
- [14] R. Anoua, S. Touhtouh, M. Rkhis, M. El Jouad, A. Hajjaji, F. Belhora, et al., "Optical and electronic properties of the natural alizarin dye: Theoretical and experimental investigations for DSSCs application," *Optical Materials*, vol. 127, p. 112113, 2022.
- [15] A. Aboulouard, B. Gultekin, M. Can, M. Erol, A. Jouaiti, B. Elhadadi, et al., "Dye sensitized solar cells based on titanium dioxide nanoparticles synthesized by flame spray pyrolysis and hydrothermal sol-gel methods: A comparative study on photovoltaic performances," *Journal of Materials Research and Technology*, vol. 9, no. 2, pp. 1569-1577, 2020.
- [16] L. Filipovic, S. Selberherr, G. C. Mutinati, E. Brunet, S. Steinhauer, A. Köck, et al., "Methods of simulating thin film deposition using spray pyrolysis techniques," *Microelectronic Engineering*, vol. 117, pp. 57-66, 2014.
- [17] L. N. Dang Quang, A. K. Kaliyamurthy, N. H. Hao, "Co-sensitization of metal based N719 and metal free D35 dyes: An effective strategy to improve the performance of DSSC," *Optical Materials*, vol. 111, p. 110589, 2021.
- [18] G. Kiruthiga Prabhu, T. Raguram, K. S. Rajni, "Annealing effect of magnesium tin oxide thin films prepared by nebulizer spray pyrolysis technique for DSSC applications," in *IOP Conference Series: Materials Science and Engineering*, vol. 577, p. 012093, 2019.
- [19] S. Kalaiselvan, K. Balachandran, S. Karthikeyan, R. Venckatesh, "Botanical hydrocarbon sources based MWCNTs synthesized by spray pyrolysis method for DSSC applications," *Silicon*, vol. 10, no. 2, pp. 211-217, 2018.
- [20] S. Sujono, Z. Arifin, "Sistem kontrol otomatis suhu dan kelembapan pada budidaya jamur tiram berbasis IoT," *Exact Papers in Compilation*, vol. 4, no. 3, pp. 585-590, 2022.
- [21] S. Abid, M. J. Irshad, M. Wasif, Z. Mehmood, I. Hussain, M. H. Ejaz, "Location-assistive and real-time query IoT-based transport system," *Engineering Proceedings*, vol. 12, p. 101, 2021.
- [22] T. Ohno, K. Sarukawa, K. Tokieda, M. Matsumura, "Morphology of a TiO<sub>2</sub> photocatalyst (Degussa, P-25) consisting of anatase and rutile crystalline phases," *Journal of Catalysis*, vol. 203, no. 1, pp. 82-86, 2001.
- [23] V. A. González-Verjan, B. Trujillo-Navarrete, R. M. Félix-Navarro, J. N. Díaz de León, J. M. Romo-Herrera, J. C. Calva-Yáñez, et al., "Effect of TiO<sub>2</sub> particle and pore size on DSSC efficiency," *Materials for Renewable and Sustainable Energy*, vol. 9, no. 2, pp. 1-8, 2020.
- [24] HiSoUR, "Dye-sensitized solar cell – Hi so you are," [Online], Jan 13, 2023. Available: <https://www.hisour.com/dye-sensitized-solar-cell-39656/>
- [25] S. Nur, Y. Kamaru, M. K. Ahmad, "Transparent dye-sensitized solar cell using titanium dioxide thin film," *Evolution in Electrical and Electronic Engineering*, vol. 3, no. 2, pp. 108-117, 2022.
- [26] J. Liu, Y. Li, S. Arumugam, J. Tudor, S. Beeby, "Screen printed dye-sensitized solar cells (DSSCs) on woven polyester cotton fabric for wearable energy harvesting applications," *Materials Today Proceedings*, vol. 5, no. 5, pp. 13753-13758, 2018.



- [27] S. K. Dhungel, J. G. Park, "Optimization of paste formulation for TiO<sub>2</sub> nanoparticles with wide range of size distribution for its application in dye sensitized solar cells," *Renewable Energy*, vol. 35, no. 12, pp. 2776-2780, 2010.
- [28] T. A. Ruhane, M. Tauhidul Islam, M. Saifur Rahaman, M. M. H. Bhuiyan, J. M. M. Islam, T. I. Bhuiyan, et al., "Impact of photo electrode thickness and annealing temperature on natural dye-sensitized solar cell," *Sustainable Energy Technologies and Assessments*, vol. 20, pp. 72-77, 2017.